


CD29 targeted near-infrared photoimmunotherapy (NIR-PIT) in the treatment of a pigmented melanoma model

Aki Furusawa , Ryuhei Okada, Fuyuki Inagaki, Hiroaki Wakiyama, Takuya Kato, Hideyuki Furumoto, Hiroshi Fukushima, Shuhei Okuyama, Peter L. Choyke, and Hisataka Kobayashi

Molecular Imaging Branch, Center for Cancer Research, National Cancer Institute, Bethesda, Maryland, USA

ABSTRACT

Near-infrared photoimmunotherapy (NIR-PIT) is a newly developed cancer treatment that utilizes an antibody-photoabsorber-conjugate (AbPC) combined with NIR light. The AbPC is injected and binds to the tumor whereupon NIR light irradiation causes a photochemical reaction that selectively kills cancer cells. NIR-PIT is ideal for surface-located skin cancers such as melanoma. However, there is concern that the pigment in melanoma lesions could interfere with light delivery, rendering treatment ineffective. We investigated the efficacy of CD29- and CD44-targeted NIR-PIT (CD29-PIT and CD44-PIT, respectively) in the B16 melanoma model, which is highly pigmented. While CD29-PIT and CD44-PIT killed B16 cells *in vitro* and *in vivo*, CD29-PIT suppressed tumor growth more efficiently. Ki67 expression showed that cells surviving CD29-PIT were less proliferative, suggesting that CD29-PIT was selective for more proliferative cancer cells. CD29-PIT did not kill immune cells, whereas CD44-PIT killed both T and NK cells and most myeloid cells, including DCs, which could interfere with the immune response to NIR-PIT. The addition of anti-CTLA4 antibody immune checkpoint inhibitor (ICI) to CD29-PIT increased the infiltration of CD8 T cells and enhanced tumor suppression with prolonged survival. Such effects were less prominent when the anti-CTLA4 ICI was combined with CD44-PIT. The preservation of immune cells in the tumor microenvironment (TME) after CD29-PIT likely led to a better response when combined with anti-CTLA4 treatment. We conclude that NIR-PIT can be performed in pigmented melanomas and that CD29 is a promising target for NIR-PIT, which is amenable to combination therapy with other immunotherapies.

ARTICLE HISTORY

Received 31 July 2021
Revised 14 December 2021
Accepted 14 December 2021

KEYWORDS

Cancer; near-infrared photoimmunotherapy (NIR-PIT); target molecule; melanoma; CD29

Introduction

Near-infrared photoimmunotherapy (NIR-PIT) is a newly developed cancer therapy that utilizes an antibody-photoabsorber-conjugate (AbPC) and NIR light. The photoabsorber dye IRDye700DX (IR700) is conjugated to a monoclonal antibody (mAb) directed against overexpressed tumor receptors on the cancer cell surface. AbPCs are intravenously injected and bind to target antigens on the cancer cell surface. After an appropriate amount of time for accumulation (typically 24 hours), NIR light (at 690 nm) is applied. IR700 is unique in that prior to light exposure it is highly hydrophilic but after light exposure, photoinduced ligand release causes a dramatic change in solubility and the remaining molecule becomes highly hydrophobic. This, in turn, leads to aggregation of the antibody-antigen complex causing damage to the cell membrane. Within a minute of the exposure of NIR light cells begin to swell, bleb and rupture, leading to necrotic/immunogenic cell death. The process is highly selective with minimal or no damage to non-expressing normal cells.¹

One of the advantages of NIR-PIT is that it is relatively noninvasive. Although light can be delivered interstitially through light fibers, the ideal lesion is one that is on the skin surface and can be irradiated directly. For this reason, NIR-PIT is thought to be ideal for the treatment of skin cancers such as

melanoma. However, there is concern that the pigment within most melanomas could absorb light interfering with NIR-PIT. While non-pigmented melanoma has been treated with NIR-PIT² preclinically, there is no experience with pigmented lesions. Although the absorption of NIR light by melanin pigment is relatively small³ and not likely to largely affect the treatment, this question is of translational relevance since the majority of melanoma cases are pigmented.⁴ Thus, in this study, we employed the B16 melanoma model, which is highly pigmented. We also used MOC2 (mouse oral cancer 2) tumor model, which is not pigmented, as a comparison.

Another advantage of cancer-cell targeted NIR-PIT is that the therapy induces anti-cancer immune activation. The rapid destruction of cancer cells by NIR-PIT releases intact antigens in the treatment site, which induces dendritic cell (DC) maturation followed by DC-mediated CD8 T cell activation.⁵ In order to maximize such immune activation, the targets for NIR-PIT have to be chosen carefully considering its expression on the immune cells in the tumor microenvironment (TME) as well as on cancer cells.

There are a limited number of tumor antigens on melanomas suitable for targeting with NIR-PIT. In this study, we tested the efficacy of CD44- and CD29- targeted NIR-PIT (CD44-PIT and CD29-PIT, respectively). CD44 is a non-

kinase transmembrane glycoprotein known to be overexpressed in many kinds of cancers such as pancreatic cancer^{6,7} and breast cancer.⁸ The overexpression of CD44 is associated with a poor prognosis.⁶ CD44 expression is known to be associated with stemness^{9,10} and drug resistance.⁷ CD44-PIT has been shown to be effective in multiple murine tumor models.^{11–13} However, many tumor models have very little or no CD44 expression.¹² Also, CD44 is highly expressed in immune cells in the TME such as activated T cells and DCs¹⁴ which activates T cells, and our previous study showed that CD44-PIT killed both T cells and cancer cells¹⁵ thus, interfering with the immune response to NIR-PIT. Damaging immune cells in the TME is counterproductive as it interferes with the overall response to NIR-PIT. Nonetheless, CD44-PIT has been combined with other immunotherapies such as immune checkpoint inhibitors (ICIs) which improve overall efficacy.^{12,15–17} However, damage to immune cells in the TME is clearly a disadvantage of using CD44 as a target. Therefore, we sought an additional target candidate for NIR-PIT which is commonly expressed in cancer cells but is not highly expressed in immune cells.

CD29, also known as Integrin beta-1 (Itgb1), is one of the integrin family trans-membrane proteins which is involved in multiple cellular events such as cell adhesion and migration.¹⁸ CD29 expression is associated with cancer cell proliferation and migration,^{19,20} and is also associated with poor prognosis in breast cancer patients.²¹ CD44 and CD29 are known to be co-expressed in some cancers including synovial sarcoma²² and squamous cell carcinomas¹⁹ and melanomas.^{23,24} Although CD29 is known to be expressed in cytotoxic T cells,²⁵ its expression in other immune cells is relatively low.²⁶ Even when cytotoxic CD8 T cells are killed locally in the treatment site, if the rest of the immune cell populations such as DCs and CD4 T cells are intact, anti-tumor immune activation is expected to be unaffected, and newly activated T cells would fill the loss. Thus, in this study, we investigated the effect of CD29- and CD44-PIT on cancer cells and on TME cells. Specifically, we investigated; (1) the efficacy of NIR-PIT against a pigmented melanoma model and (2) Compared the treatment efficacy of CD29-PIT and CD44-PIT with and without a commonly available immune checkpoint inhibitor, anti-CTLA4 antibody.

Materials and methods

Synthesis of AbPC

One milligram (6.7 nmol) of anti-CD29 and anti-CD44 antibodies (clone KM16 and IM7, respectively, purchased from Bio X Cell) were incubated with 66.8 µg (34.2 nmol) of IR700 NHS ester (Li-Cor) in 0.1 M Na₂HPO₄ solution (pH 8.5) for 1 hour at room temperature. The mixture was purified using a PD-10 Desalting Column with Sephadex G-25 resin (Cytiva) and eluted with PBS. The resulting AbPC solution was diluted to make 1.675 nmol/mL. AbPCs were analyzed by SDS-PAGE with a 4–20% gradient polyacrylamide gel (Life Technologies). The same amount of unconjugated antibodies were loaded next to the AbPCs as controls. The

gel was imaged with a Pearl Imager (LI-COR Biosciences) using a 700 nm fluorescence channel. The gel was stained with Colloidal Blue staining to determine the molecular weight of AbPCs.

Cell culture

B16-F10 (abbreviated as B16) was a kind gift from Dr. Samuel Hwang (NCI, Dermatology Branch), MOC2 was purchased from Kerafast. B16 cells were cultured in RPMI1640 media (Thermo Fisher Scientific) supplemented with 10% fetal bovine serum (FBS, Thermo Fisher Scientific) and 100 I.U./mL penicillin and 100 µg/mL streptomycin (Thermo Fisher Scientific). MOC2 cells were cultured in the 1:1 mixture of IMDM medium and Ham's Nutrient Mixture F12 Media (GE Health Healthcare Life Sciences) supplemented with 5% FBS, 100 I. U./mL penicillin and 100 µg/mL streptomycin, 5 ng/mL insulin (MilliporeSigma), 40 ng/mL hydrocortisone (MilliporeSigma), and 3.5 ng/mL human recombinant EGF (MilliporeSigma). All cells were cultured in a humidified incubator at 37°C in an atmosphere of 95% air and 5% CO₂ for no more than 30 passages.

In vitro expression analysis by flow cytometry

B16 cells were seeded in a 24 well plate at 0.1×10^6 cells/well (dilution 1), 0.025×10^6 cells/well (dilution 4), at 0.00625×10^6 cells/well (dilution 16). After 2 days of culture when the dilution 1 culture was fully confluent, cells were collected with trypsin and stained with either anti-CD29-PE (clone HMβ1-1, Thermo Fisher Scientific), anti-CD44-PE (clone IM7, Thermo Fisher Scientific), Armenian hamster IgG-PE (clone eBio299Arm, eBiosciences) or rat IgG2bκ-PE (clone RTK4530, Biolegend) then fixed and permeabilized with Foxp3/Transcription Factor Staining Buffer Set (Thermo Fisher Scientific) and stained with anti-Ki67-APC (clone 10A8, Biolegend). Cells were analyzed with flow cytometry (FACSLyric, BD Biosciences) and Flowjo software (BD Biosciences).

FACS analysis of AbPC binding to B16 cells

B16 cells were cultured in tissue culture flasks (182 cm²; CELLTREAT Scientific Products) and collected when cells were approximately 80% confluent. 0.2×10^6 cells were collected in 100 µL PBS and incubated with 1 µg AbPCs at 4°C for 1 hour. For the blocking controls, 10 µg (10 × excess amount of AbPC) unlabeled antibodies were added 1 hour prior to the incubation with AbPC. The stained cells were analyzed with flow cytometry (FACSLyric, BD Biosciences) and Flowjo software (BD Biosciences).

In vitro NIR-PIT and MTT assay

B16 cells were seeded in a 24 well plate at 0.1×10^6 cells/well a day before the experiment, 1 µg AbPC was added to each well and incubated at 37°C for 1 hour. Media was replaced with fresh phenol-red-free RPMI medium. The cells were irradiated with NIR light with an ML7710 laser system (Modulight) at 150 mW/

cm² for various lengths of time so that the total light dose was 0, 5, 20, 50 J/cm². The cells were incubated for another 3 hours then media was replaced with 500 µL of 3-(4,5-Dimethyl-2-thiazolyl)-2,5-diphenyl-2 H-tetrazolium bromide (MTT) reagent (0.5 mg/mL, SIGMA Aldrich) and incubated for 1 hour at 37°C. The supernatant was discarded, and the crystal formazan dye was dissolved in 500 µL of 2-propanol. The absorbance was measured at 570 nm on a microplate reader (800 TS; BioTek).

Animal models

B6 albino 6–10 week old female mice were purchased from Charles River Laboratories. All procedures were performed in compliance with the Guide for the Care and Use of Laboratory Animals and approved by the local Animal Care and Use Committee. One million B16 cells or MOC2 cells were subcutaneously injected into the upper thigh of the animals. The hair around the injection site was removed prior to the tumor inoculation. Mice were monitored each day, and tumor volumes were assessed 3 times a week by caliper and calculated using the following formula: tumor volume (mm³) = length × width² × 0.5. The mice were euthanized with CO₂ when the tumor volume reached 2000 mm³. Tumor-bearing mice were used seven days after the inoculation.

In vivo NIR-PIT

For the comparison of CD29-PIT and CD44-PIT, B16 tumor-bearing mice were grouped as follows: (i) no treatment (control), (ii) anti-CD29-IR700 i.v. injection only (AbPC only), (iii) anti-CD29-IR700 i.v. injection followed by NIR light irradiation (CD29-PIT) (iv) anti-CD44-IR700 i.v. injection followed by NIR light irradiation (CD44-PIT). For the AbPC only and PIT groups, AbPCs (0.335 nmol in 200 µL PBS) were intravenously injected a day prior to NIR light irradiation (day -1). For testing the combination of anti-CTLA4 administration and CD29-PIT or CD44-PIT, the B16 tumor bearing mice were grouped as follows: (i) no treatment (control), (ii) anti-CTLA4 (clone 9D9, Bio X Cell) i.p. injection only (aCTLA4 only), (iii) anti-CTLA4 administration plus CD29-PIT (aCTLA4+ CD29-PIT), (iv) anti-CTLA4 administration plus CD44-PIT (aCTLA4+ CD44-PIT). NIR light was irradiated with an ML7710 laser system (Modulight) at either 50 J/cm² at 150 mW/cm² or 20 J/cm² at 70 mW/cm², for either one time (at day 0) or two times (at day 0 and 1). The mice were covered with aluminum foil with an approximately 10 mm diameter hole through which NIR light was irradiated. For Kaplan–Meier survival analysis, the endpoint was set as tumor size above 2000 mm³ at which point the mice were euthanized.

Histology analysis

The PIT-treated tumors were harvested either 1 hour or 1 day after the NIR light irradiation. The FFPE sections were stained with hematoxylin and eosin (H-E).

Multiplex immunohistochemistry (IHC)

Multiplex IHC was performed as previously described,¹⁷ using Opal Automation IHC Kit (Akoya Bioscience) and Bond RXm autostainer (Leica Biosystems). The following antibodies were

used: anti-CD29 (EPR16895; Abcam; 1:1000 dilution), anti-CD44 (clone IM7, Bio X Cell; 1:1000 dilution), anti-gp100 (clone EP4863(2); Abcam; 1:1000 dilution), anti-MelanA (clone EPR20380; Abcam, 1:1000 dilution), anti-CD8 (clone EPR20305; Abcam; 1:500 dilution), anti-CD4 (clone EPR19514; Abcam; 1:1000 dilution), anti-Foxp3 (clone 1054 C; Novus Biologicals; 1:1,000 dilution), anti-Ki67 (clone D3B5; Cell Signaling Technology; 1:1000 dilution), anti-DIG (clone 9H27L19; Thermo Fisher Scientific; 1:500 dilution), anti-CD31 (clone D8V9E; Cell Signaling Technology; 1:500 dilution). Stained slides were mounted with ProLong Diamond Antifade Mountant (Thermo Fisher Scientific) and imaged with Mantra Quantitative Pathology Workstation (Akoya Biosystems). The images were analyzed with inForm Tissue Finder software and phenoptrReports (Akoya Biosystems). For T cell counting, the tissue area was segmented into “Stroma” and “Tumor” based on the expression of gp100 and MelanA. Cell phenotypes were identified via machine-learning algorithms based on the following criteria: cancer cells (gp100+, MelanA+, CD45-), CD8 T cells (CD45+, CD3+, CD8+), endothelial cells (CD31+, CD45-). At least five images were obtained for each specimen, and tissue area and cell count were summed for each tissue category. Cell density was calculated as cell counts per square millimeter. For the Ki67 positive percentage calculation, the area of PIT survivor tumor tissue and the edge region of control tumors were manually segmented and the Ki67 positive percentage among cancer cells was calculated using the scoring function of inForm.

DIG-labeled antibody detection by IHC

The labeling of antibodies with digoxigenin (DIG) was performed similarly as IR700 conjugation using 1 mg of anti-CD29, anti-CD44 or isotype rat IgG2b (clone KM16, IM7, and LTF-2, respectively, all purchased from Bio X Cell) and 50 µg of digoxigenin succinimidyl ester (Thermo Fisher Scientific). The resulting DIG-labeled antibodies were abbreviated as anti-CD29-DIG, anti-CD44-DIG, and isotype-DIG, respectively. Each DIG-labeled antibody (0.335 nmol in 200 µL PBS) was injected intravenously into tumor-bearing mice, tumors and contralateral skin were harvested a day later. The distribution of labeled antibodies was detected in FFPE sections by anti-DIG IHC using anti-DIG (clone 9H27L19; ThermoFisher Scientific).

In situ TUNEL assay

In situ TUNEL assay was performed with Click-iT Plus TUNEL Assay with Alexa488 (Thermo Fisher Scientific). The FFPE sections of tumors were processed per manufacturer-recommended protocol. DAPI was used to stain nuclear DNA.

Ex-vivo NIR-PIT

Single-cell suspension from one tumor was split into five tubes (for control, CD29-PIT, CD44-PIT, IgG2a-PIT, and IgG2b-PIT) and incubated with 2.5 µg of either AbPC in 1 mL media in 37°C for one hour. Cells were then washed and moved to 12 well plates in 1 mL phenol red-free RPMI

media. 20 J/cm² NIR light was applied at 70 mW/cm², then cells were immediately stained with antibodies and analyzed by flow cytometry.

FACS analysis of tumor and LN

Single-cell suspension was obtained as previously described.¹⁵ The cells were stained with the following antibodies: anti-CD3e (145–2 C11), anti-CD8α (53–6.7), anti-CD11b (M1/70), anti-CD11c (N418), anti-CD25 (PC61.5), anti-F4/80 (BM8), anti-CD45 (30-F11), anti-Ly-6G (1A8), anti-Ly-6C (HK1.4), anti-CD31 (390), anti-I-A/I-E (M5/114.15.2), anti-ratIgG2ak (RTK2758) and anti-ratIgG2bκ (RTK4530) from Biolegend or anti-CD4 (RM4-5), anti-CD69 (H1.2F3), anti-Klrg1 (2F1), anti-CD80 (16–10A1) and anti-NK1.1 (PK136) from ThermoFisher Scientific. Cells were also stained with Fixable Viability Dye (Thermo Fisher Scientific) and dead cells were gated out from the analysis. The stained cells were analyzed with flow cytometry (FACSLyric, BD Biosciences) and Flowjo software (BD Biosciences). Cell types were determined as following; CD8 T cells: CD45+/ CD3+/ CD8+, CD4 T cells: CD45+/ CD3+/ CD4+, NK cells: CD45+/ CD3-/ NK1.1+, DC1: CD45+/ CD11b-/ CD11c+, DC2: CD45+/ CD11b+/ CD11c+, EC: CD45-/ CD31+, CC: ssc high/ fsc high/ CD45-, MDSC: CD45+/ CD11b+/ Ly6G+ or Ly6C+, TAN: CD45+/ CD11b+/ Ly6G+, TAM: CD45+/ CD11b+/ F4/80 +.

Statistical analysis

Statistical analysis was performed using GraphPad Prism (GraphPad Software). n = number of independent experiments. A P-value of less than 0.05 was considered significant.

Result

CD29 and CD44 targeted PIT kill B16 melanoma cells

We tested the surface expression of CD29 and CD44 in B16 melanoma cells cultured at various densities. Flowcytometry was performed when the highest density culture (dilution 1) was fully confluent and lower density cultures (dilution 4 and 16) were in a growing phase. Ki67 expression level was negatively correlated with cell density, showing that cells were actively proliferating in lower density cultures. CD29 expression negatively correlated with cell density, whereas CD44 expression positively correlated with cell density (Figure 1 (a)). This expression pattern suggested that CD29 expression was higher in the more proliferative subset of B16 cells, while CD44 expression was higher in the less proliferative subset of B16 cells. Next, anti-CD29 and anti-CD44 were conjugated with IR700 to generate AbPCs (anti-CD29-IR700 and anti-CD44-IR700, respectively). The conjugation of IR700 was validated by SDS-PAGE (Figure 1(b)). Both AbPCs showed similar fluorescent intensity in 700 nm fluorescence, suggesting the conjugation efficiency was similar for these AbPCs. The binding of each AbPC to B16 cells was analyzed by flowcytometry (Figure 1(c)). When bound to the target, there was a fluorescence shift in the IR700 signal and this shift was diminished when the AbPC was blocked with excess unlabeled

antibody showing the binding capability of antibodies to the target cells was not altered due to IR700 conjugation. In order to see if the AbPC binding is cell type specific, we also tested AbPC binding to BALB/3T3 fibroblast cell line (Supplemental Fig. 1). CD29-IR700 did not bind to BALB/3T3 cells, whereas CD44-IR700 bound to BALB/3T3 cells, suggesting that anti-CD29 binding to B16 was cell type specific, and anti-CD44 may also bind to fibroblasts besides B16 melanoma cells.

In order to test the efficacy of cell killing by CD29 and CD44 targeted NIR-PIT (CD29-PIT and CD44-PIT, respectively), cell viability was tested by the MTT assay 3 hours after *in vitro* NIR-PIT (Figure 1(d)). Both agents killed B16 melanoma cells in a light dose-dependent manner. CD44-PIT completely killed B16 cells at 20 J/cm², whereas CD29-PIT killed about half the B16 cells with 50 J/cm² NIR light.

In vivo cancer cell killing with CD29-PIT and CD44-PIT in established tumors

We tested the expression of CD29 and CD44 in established B16 melanomas using multiplex IHC (Figure 2(a)). CD29 expression was typically uniform throughout the entire tumor, including the edge, whereas CD44 was usually expressed in a gradient that diminished toward the tumor edge. CD29 expression was seen both in the cytoplasm and on the cell membrane, whereas CD44 expression was seen only on the cell membrane. To assess the antibody delivery to the target cells, digoxigenin (DIG) was conjugated to anti-CD29, anti-CD44, and isotype control rat IgG2bκ (anti-CD29-DIG, anti-CD44-DIG, and isotype-DIG, respectively) which were injected into B16 tumor-bearing mice. The tumors were collected one day later and the distribution of antibodies was analyzed by anti-DIG IHC (Figure 2(b)). Anti-CD29-DIG and anti-CD44-DIG were detected on the cell surface of B16 cells showing that AbPCs were successfully delivered to the tumor tissue and bound to cancer cell surfaces. Isotype-DIG was not detected on B16 tumor cells, showing that AbPC binding on cancer cells was specific for CD29 and CD44.

Next, we examined tissue histology by H-E staining in B16 tumors after *in vivo* CD29-PIT and CD44-PIT. AbPCs were injected 1 day prior to NIR light irradiation, which was delivered at 150 mW/cm², 50 J/cm², and treated tumors were harvested 1 hour or 1 day post NIR light irradiation. In the case of tumors evaluated 1 hour post NIR light irradiation, B16 tumor cells from both CD29-PIT and CD44-PIT treated samples showed condensed nuclei and ruptured membranes which are the typical morphology of necrotic cells.²⁷ The affected areas spanned approximately 3–4 mm deep from the surface (Supplemental Fig. 2). Within the affected area, dilation of blood vessels and gapping between cells were observed. These features have been previously described²⁸ after successful NIR-PIT treatment in other tumors. One day post PIT, PIT-treated tumor cells appeared nearly completely necrotic, with a small portion of surviving cells at the farthest side from the surface, showing both CD29-PIT and CD44-PIT successfully killed B16 tumor cells *in vivo*. Tumors exposed to NIR light alone showed

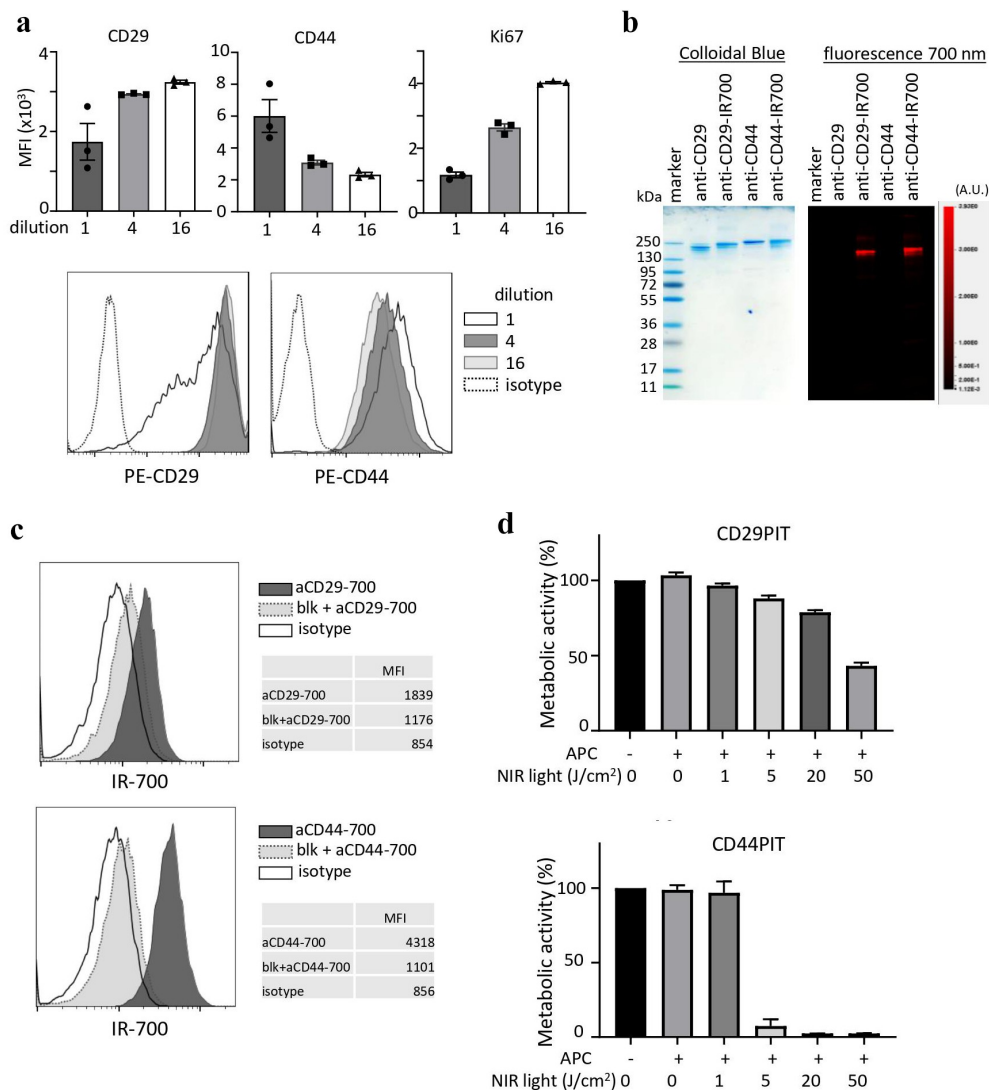


Figure 1. CD29 and CD44 targeted PIT kill B16 melanoma cells *in vitro*. (a) Surface expression of CD29 and CD44, and nuclear expression of Ki67 were tested in B16 cells cultured in various densities. Cells were analyzed by flow cytometry when dilution 1 (0.1×10^6 cells/well) culture was full confluent and dilution 4 and 16 (0.025×10^6 cells/well and 0.0625×10^6 cells/well) cultures were rapidly dividing. The bar graphs show MFI (median fluorescent intensity) from 3 replicate wells and are shown as mean \pm SEM. The histograms show the representative CD29 and CD44 expressions compared to isotype controls. (b) Validation of IR700 conjugation to anti-CD29 and anti-CD44 by SDS-PAGE. The left panel shows colloidal Blue staining, the right panel shows 700 nm fluorescence of IR700. The same amount of unconjugated antibody was used as control. (c) The binding of anti-CD29-IR700 (aCD29-700) or anti-CD44-IR700 (aCD44-700) to B16 cells was tested by flow cytometry. B16 cells were incubated with IR700-labeled anti-CD29 or anti-CD44 with or without blocking (blk) with excess unlabeled antibody. The experiments were repeated twice, the representative histograms are shown. (d) MTT assay to test the cell-killing efficacy of CD29-PIT and CD44-PIT against B16 cells. CD29 and CD44 targeted *in vitro* PIT was performed on B16 cells, NIR light was irradiated at 150 mW/cm^2 in indicated doses. Cell metabolic activity was measured by MTT assay 3 hours after NIR light irradiation, shown as % vs control (ab-/0 J). The representative example from 3 experiments was shown. (5 replicate wells, shown as mean \pm SEM).

normal morphology, suggesting that the cancer cell killing by CD29-PIT and CD44-PIT were PIT-target specific, not by NIR light alone.

Besides histology, we also tested cell death by detecting damaged DNA using TUNEL staining (Figure 2(c)). In the untreated control tumor, only occasional brightly labeled nuclei representing apoptotic cells were observed. On the other hand, both CD29-PIT and CD44-PIT treated tumors showed dimly stained nuclei representing necrotic cells throughout the tumor and only a small portion of TUNEL-negative live cells on the tumor edge. We did not detect TUNEL staining at 1 hour post PIT (data not shown), suggesting that DNA damage was not apparent even though cell membrane damage had already occurred.

In order to evaluate the effect of NIR light dose, CD29-PIT and CD44-PIT were performed with different light doses and tissue histology was examined with H-E staining (supplemental table 1). With a high dose of NIR light, (50 J/cm^2 NIR light using 150 mW/cm^2 laser), the majority of CD29- and CD44-PIT treated tumors were entirely necrotic. However, at this light dose, we observed occasional adverse events such as paralysis of the extremity (data not shown). With one-time irradiation of low-dose NIR light with low power laser output (20 J/cm^2 using 70 mW/cm^2 laser), none of the tumors showed diffuse necrosis. However, with two times irradiation of low-dose NIR light, half of CD29-PIT treated tumors were entirely necrotic and the remainder were partially necrotic while CD44-PIT resulted mostly in partial tumor cell death. Although this degree of cell damage may not be enough to shrink

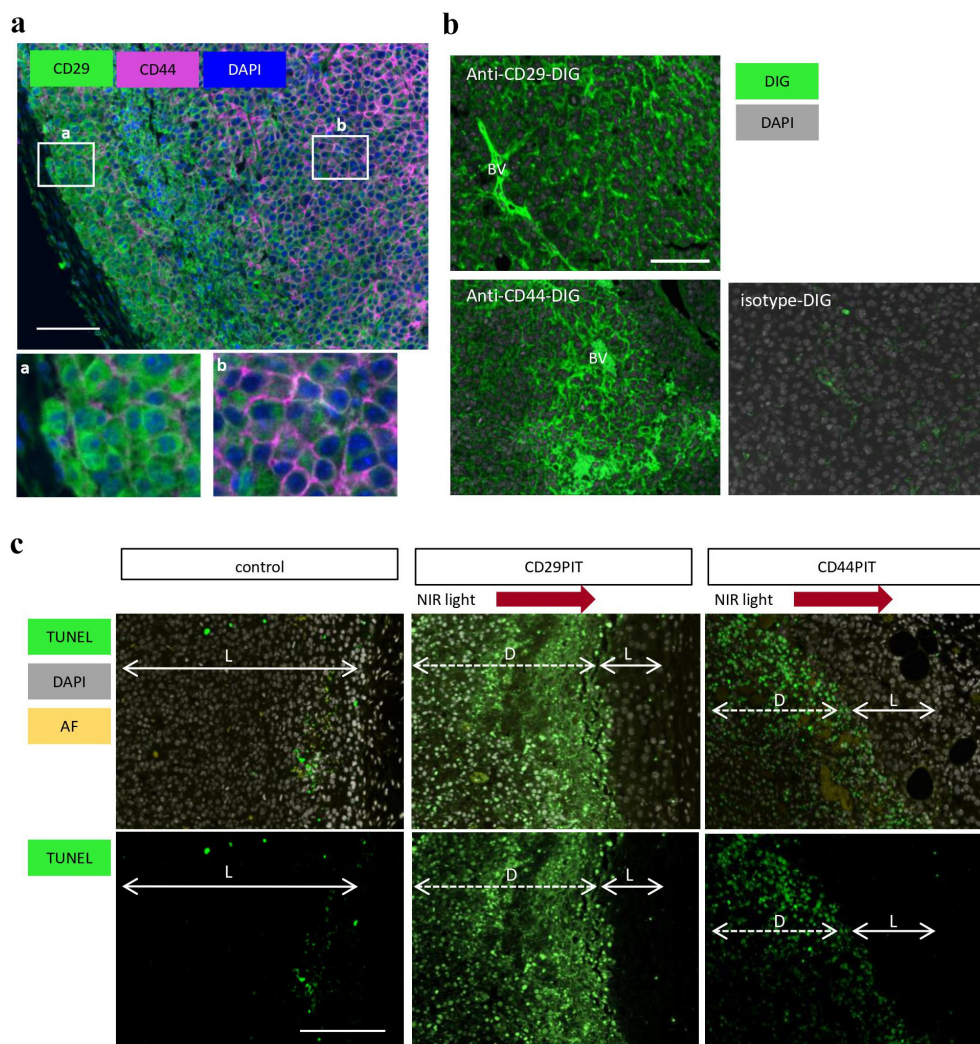


Figure 2. Expression of CD29 and CD44 in established B16 tumors and cell killing by NIR-PIT. (a) Representative example of CD29 and CD44 expression in B16 tumor detected with multiplex IHC. Insets (a and b) are enlarged on the bottom. (b) The distribution of DIG-labeled anti-CD29 and anti-CD44 was detected by anti-DIG IHC in B16 tumors. BV = blood vessel. (c) Cell death was detected by TUNEL staining 1 day after CD29-PIT and CD44-PIT with $2 \times 20 \text{ J/cm}^2$ 70 mW/cm^2 NIR light. Arrows with solid line indicate TUNEL-negative live (L) tissue, arrows with dotted line indicate TUNEL-positive dead (D) tissue. The red arrows indicate the direction of NIR light irradiation (from left to right). AF = autofluorescence, scale bar = $100 \mu\text{m}$.

tumors, it should be enough to induce anti-tumor immune activation. Therefore, we used $2 \times 20 \text{ J/cm}^2$ NIR light for both CD29- and CD44-PIT *in vivo* for survival analysis. In order to test if the tumor cell death induced by NIR-PIT is affected by the pigment of the tumor, we also tested CD29-PIT and CD44-PIT on the MOC2 tumor model (Supplemental Fig. 3). MOC2 tumor has a similar expression pattern of CD29 and CD44 as B16 melanoma but does not have pigment in its cells (Supplemental Fig. 3A). In MOC2 tumors, necrosis was observed after CD29-PIT and CD44-PIT. The affected area often extended 3–4 mm deep from the surface, which was similar to the result in the B16 model. These results suggested that the pigment in the cells does not diminish the cell killing efficacy of NIR-PIT.

The effect of CD29-PIT and CD44-PIT on non-cancer tissues

Next, we evaluated cell surface expression of CD29 and CD44 in non-cancer tissues such as the vasculature and normal skin surrounding the B16 tumor. CD29 is known to be expressed in

endothelial cells (ECs).²⁹ We observed that CD29 is highly expressed in CD31-positive ECs in both large blood vessels and capillaries (Supplemental Fig. 4A). Although vascular expression of CD44 was not detectable by IHC in B16 tumors in this study (Supplemental Fig. 4A), CD44 is known to be expressed in ECs and has a role in vasculature development.^{29,30} Vascular EC death was assessed by TUNEL staining after CD29-PIT and CD44-PIT with 50 J/cm^2 NIR light at 150 mW/cm^2 . In the affected tumor area, TUNEL-positive dead cells were detected in the blood vessels in both CD29-PIT and CD44-PIT treated tumors (Supplemental Fig. 4B). However, the frequency of TUNEL-positive blood vessels was not high and notable bleeding was not detected, suggesting that the physical structure of blood vessels was maintained after CD29- and CD44-PIT.

Next, we tested the effect of CD29-PIT and CD44-PIT on normal skin. Both CD29 and CD44 are known to be expressed in the epidermis in both humans and mice.^{31–36} IHC showed that CD29 and CD44 are expressed in the

epidermis and hair follicles, while CD44 was more widely expressed in the epidermis (Supplemental Fig. 5A). The antibody delivery was confirmed with DIG-labeled antibodies. In both anti-CD29-DIG and anti-CD44-DIG injected mice, DIG was rarely detected in the epidermis nor in the hair follicle despite the expression of the antigens at these sites (Supplemental Fig. 5B). This indicated that the antibodies did not penetrate deeply into the epidermis. All the tested antibodies including isotype-DIG were detected in the dermis. This was thought to represent a nonspecific accumulation of antibodies in the extracellular matrix. This nonspecific antibody accumulation in the dermis was observed in the normal skin (non-tumor bearing skin) as well. We also performed CD29-PIT and CD44-PIT against normal skin. TUNEL staining showed no increase in cell death (Supplemental Fig. 5C). These results suggested that both CD29-PIT and CD44-PIT are safe against normal skin.

***In vivo* CD29 and CD44 targeted NIR-PIT**

Next, we performed *in vivo* CD29- and CD44-PIT in the B16 mouse tumor model to assess treatment efficacy. *In vivo* experiments delivered two doses of NIR light (20 J/cm², 70 mW/cm²). After CD29-PIT, B16 tumors shrunk, and the subsequent growth was significantly suppressed whereas CD44-PIT slightly flattened tumor growth, but subsequent tumor growth was comparable to non-treatment controls (Figure 3(b,c)). Either of the IR700 conjugated antibodies *i.v.* injection alone did not affect tumor size (Figure 3(c), Supplemental Fig. 6). All the CD29-PIT treated tumors eventually grew back and none achieved complete remission (CR), so its impact on survival was minimal (Figure 3(d)). Treated tumors often developed scab-like structures that eventually either fell off after the skin underneath healed or stayed on top of the re-growing tumor. There was no detectable damage of the skin adjacent to the treated tumor within the treatment site (Figure 3(b)).

The proliferation of surviving tumor cells following NIR-PIT

While tumor cells were killed throughout the tumor after CD29-PIT and CD44-PIT, there often was a small layer of live cells left on the far surface. IHC showed that CD29 expression in CD29-PIT surviving cells was scattered and often missing surface expression, whereas CD44 expression in CD44-PIT surviving cells was often low (Figure 4(a)). These expression patterns suggested us that combined PIT targeting both CD29 and CD44 may lead to more complete tumor cell death. *In vivo* CD29 + CD44 combined PIT did not improve tumor suppression compared to CD29-PIT (Supplemental Fig. 7), implicating that the PIT survivor cells cannot be completely eradicated by these two targets. These survivor cells eventually grew back, and CD29-PIT treated tumors grew back more slowly. We tested if there was a difference in proliferation in CD29-PIT and CD44-PIT survivor cells by testing for Ki67 expression. We observed less Ki67 staining in CD29-PIT survivor cells than in CD44-PIT survivor cells or untreated tumors (Figure 4(b,c)), suggesting that CD29-PIT surviving tumor cells were less proliferative than cells surviving CD44-PIT.

CD29-PIT does not damage immune cells at the treatment site, whereas CD44-PIT kills CD4, NK and DCs

Because an intact TME is essential for the immune effects of NIR-PIT, we assessed the effect of CD29-PIT and CD44-PIT on TME cell populations which have roles in anti-cancer immunity including CD4 and CD8 T cells, NK cells, and DCs. CD29 and CD44 expression were tested in B16 tumors and the expression intensity was compared to B16 cancer cells. Immune cells arrive in the tumor via the vasculature, so the expression of the targets on ECs was also tested. CD29 was highly expressed in cancer cells, ECs, and DC2, and expression in T cells, NK cells, and DC1 were low. CD44 was also highly expressed in cancer cells and DC2, but low in EC. The CD44 expression in immune cells was relatively higher compared to

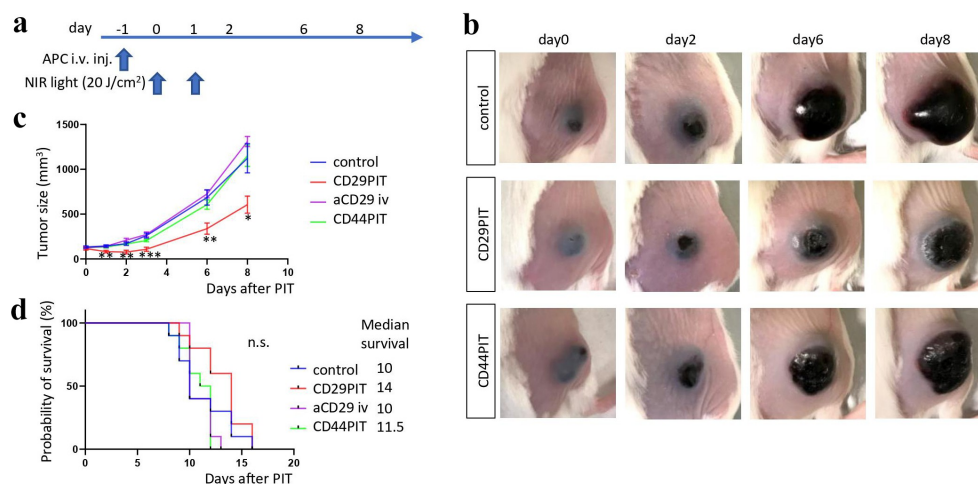


Figure 3. *In vivo* CD29- and CD44-PIT against B16 tumor model. (a) Scheme of the treatment. NIR light (20 J/cm²) was applied one and two days after APC *i.v.* injection. Pictures of tumors were taken at days 0, 2, 6, and 8. (b) representative images of tumors. (c) Tumor growth curve. aCD29 *iv* = anti-CD29-IR700 *i.v.* injection only, n = 10 (individual mice), *p < 0.05; **p < .01; ***p < .001 (vs control, one-way ANOVA followed by Tukey test) (d) Survival curve n = 10 (individual mice); n.s. not significant (vs control, log-rank test).

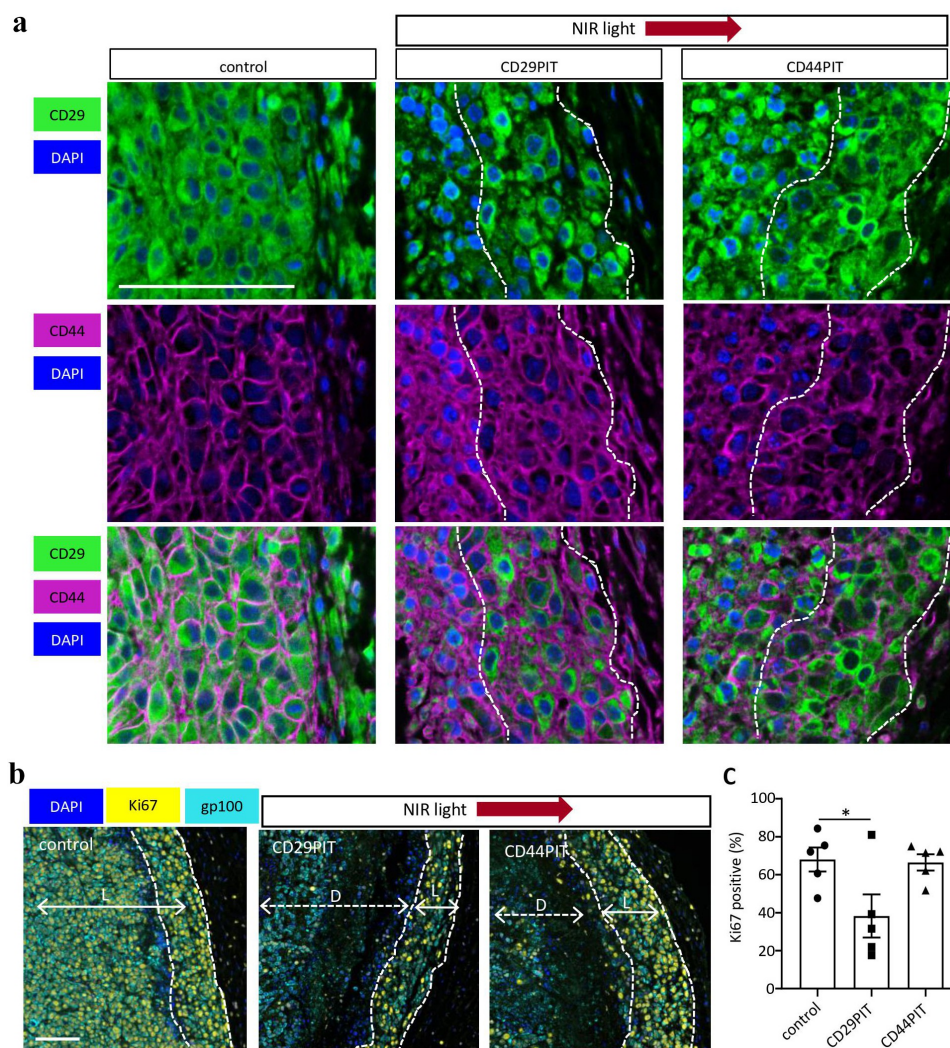


Figure 4. Proliferation marker analysis in cells surviving NIR-PIT. (a-c) CD29-PIT and CD44-PIT were performed with $1 \times$ high dose NIR light ($1 \times 50 \text{ J/cm}^2$, 150 mW/cm^2), tumors were harvested 1 day after the PIT. (a) Representative IHC images of CD29 and CD44 expression in PIT-treated B16 tumor. The areas flanked by dotted lines indicate the PIT-surviving tumor tissue. Scale bar = $100 \mu\text{m}$. (b-c) Cell proliferation of tumor cells surviving PIT was analyzed based on Ki67 expression. b. Representative IHC pictures for Ki67 expression in surviving tumor cells. The areas flanked by dotted lines indicate the PIT-surviving tumor tissue after CD29-PIT and CD44-PIT or normal tumor edge tissue in control. Arrows with solid line indicate live (L) tissue, arrows with dotted line indicate dead (D) tissue. The red arrows indicate the direction of NIR light irradiation (from left to right). (c) Percentage of Ki67+ cells in the PIT-surviving tissue and normal tumor edge. $n = 5$ (individual tumors), $*p < .05$ one-way ANOVA followed by Tukey test.

CD29 (Figure 5(a)). Next, we performed an *ex-vivo* NIR-PIT to test if CD29-PIT and CD44-PIT killed the cells that expressed these targets. In order to test nonspecific IgG on cell killing by NIR-PIT, IR700 conjugated isotype control (rat IgG2a and rat IgG2b as isotype control for anti-CD29 and anti-CD44, respectively) were also tested. Flow cytometry analysis showed that a large portion of CD45+ hematopoietic cells were lost after CD44-PIT, especially, the CD11b+ myeloid population has nearly completely disappeared (Figure 5(b)). None of the cell types were significantly killed after CD29-PIT or IgG2a-PIT. On the other hand, after CD44-PIT, CD4 T cells, NK cells, and cDC2 were significantly reduced. NK cells and DC2 were also significantly reduced after IgG2b-PIT but the reduction was smaller than after CD44-PIT (Figure 5(c,d)).

These results suggest that CD29-PIT can selectively destroy cancer cells without damaging immune cells within the treatment site, whereas CD44-PIT destroys both cancer cells and

immune cells. Slight cell reduction after IgG2b PIT suggested that nonspecific binding of AbPC, probably via the Fc receptor, can lead to cell killing and the degree of the nonspecific binding depends on the isotypes employed.

Combination therapy of CD29-PIT or CD44-PIT and anti-CTLA4 administration

Next, we tested the combination of CD29-PIT and CD44-PIT with an anti-CTLA4 immune checkpoint inhibitor (ICI). Anti-CTLA4 ICI is known to promote anti-cancer T cell activation by blocking the suppression pathway. We expected that a combination of cancer-cell targeted NIR-PIT and anti-CTLA4 ICI would augment the anti-tumor immune activation. Anti-CTLA4 was administrated on days -1, 1 and 3 (Figure 6(a)). With anti-CTLA4 ICI alone, tumor growth was slightly suppressed. With the combination of anti-

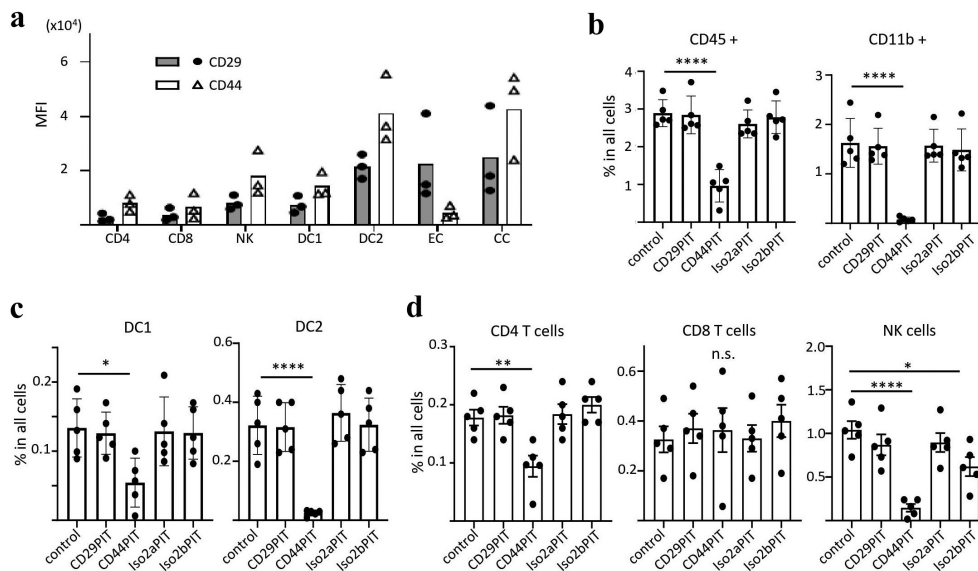


Figure 5. CD29 and CD44 expression in non-cancer cells in tumor tissue and ex-vivo NIR-PIT. (a) The surface expression of CD29 and CD44 on non-cancer cells and B16 cancer cell in B16 tumor was analyzed by flow cytometry. The expressions are shown as MFI (median fluorescent intensity). $n = 3$ (independent tumors), bars represent the average, dots represent individual samples. CD4 = CD4 T cells; CD8 = CD8 T cells; NK = NK cells; DC1 = conventional DC1; DC2 = conventional DC2; EC = endothelial cells; CC = cancer cells. (b-d) Immune cell populations in the B16 tumors were analyzed after ex-vivo PIT with anti-CD29, anti-CD44, rat IgG2a or rat IgG2b isotype control. $n = 5$ (individual tumors), *, $p < .05$; **, $p < .01$; ****, $p < .0001$; n.s., not significant (one-way ANOVA followed by Tukey test). (b) percentage of live CD45+ and CD11b+ cells in all cells. c. percentage of live DC1 and DC2 in all cells. d. Percentage of live CD4 T cells and NK cells in all cells.

CTLA4 ICI and CD29-PIT, tumor growth was clearly suppressed compared to control and anti-CTLA4 ICI alone (Figure 6(b,c)). The combination of anti-CTLA4 ICI and CD44-PIT did not show any additional effects compared to anti-CTLA4 ICI alone. The combination therapy of anti-CTLA4 ICI and CD29-PIT significantly extended survival. However, none of the mice achieved CR (Figure 6(d)). We also tested anti-PD-1 ICI in combination with CD29-PIT (supplemental Fig. 8). Although it was not statistically significant, this combination therapy also showed a similar trend of improved tumor growth suppression. However, it did not extend the long-term survival.

The combination of anti-CTLA4 ICI and CD29-PIT enhanced T cell activation and tumor infiltration

The cancer cell antigens released by immunogenic cell death after cancer cell targeted NIR-PIT induces DC maturation, followed by T cell activation, a process that often takes place in the draining lymph node (LN). We tested DC maturation, T cell activation, and effector differentiation marker expression after each treatment on day 2 (a day after the 2nd NIR light irradiation) within the draining LN (Figure 7(a)). There was no difference in CD80 expression in DCs between control and CD29-PIT, whereas CD80 expression was reduced with CD44-PIT. On

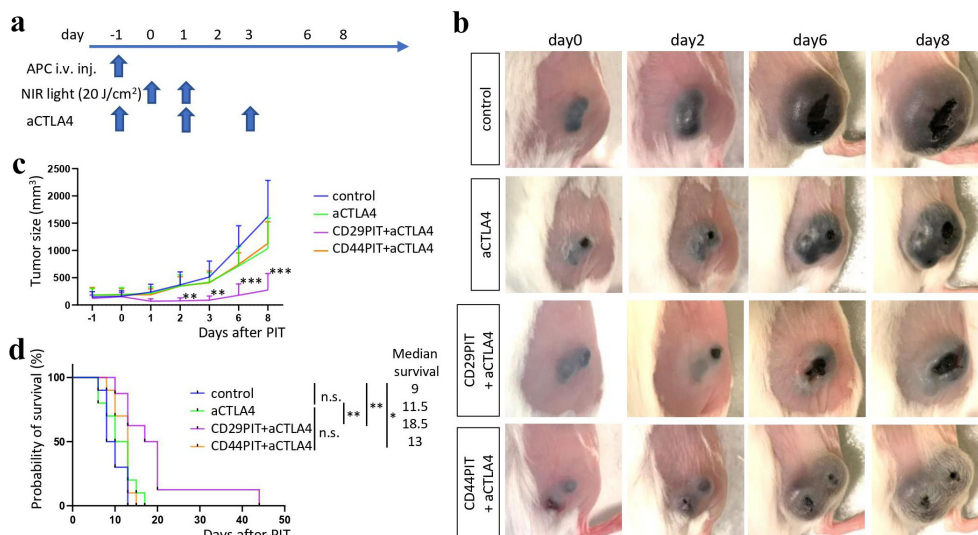


Figure 6. In vivo NIR-PIT combined with anti-CTLA4 immune checkpoint inhibitor (ICI). (a) Scheme of the treatment. NIR light (20 J/cm^2) was applied one and two days after APC iv injection. anti-CTLA4 ICI (aCTLA4) was administrated on days -1 , 1 , and 3 . Images of tumors were taken on days 0 , 2 , 6 , and 8 . (b) Representative images of tumors. (c) Tumor growth curve. $n = 10$ (individual mice); ** $p < .01$; *** $p < .0001$ (vs control, one-way ANOVA followed by Tukey test) (d) Survival curve. $n = 10$ (individual mice); * $p < .05$; ** $p < .01$ (log-rank test). Median survival: control 9, aCTLA4 11.5, CD29PIT+aCTLA4 18.5, CD44PIT+aCTLA4 13. n.s., not significant.

the other hand, the combination of anti-CTLA4 and CD29-PIT increased CD80 expression. These results suggested CD44-PIT led to impaired DC maturation, whereas anti-CTLA4 ICI + CD29-PIT promoted DC maturation, an important preliminary step to immune activation. Monotherapy of CD29-PIT and CD44-PIT both increased CD69 positive-activated CD8 T cells. Anti-CTLA4 ICI alone also increased CD69 positive activated CD8 T cells, and the combination with CD29-PIT or CD44-PIT further increased the activation of CD8 T cells (Figure 7(a) and Supplemental Fig. 9). The percentage of Klrp1 positive CD8 T cells increased after CD29-PIT monotherapy and anti-CTLA4 ICI + CD29-PIT, suggesting that CD29-PIT promoted the effector differentiation of CD8 T cells.

Next, tumor infiltration of T cells was tested 7 days after PIT. IHC showed that the number of CD8 T cells within the tumor increased after anti-CTLA4 ICI alone and anti-CTLA4 + CD29-PIT, whereas the increase was not significant after anti-CTLA4

+ CD44-PIT (Figure 7(b,c)). Cell proliferation marker expression in tumor cells revealed fewer Ki67 positive cancer cells after anti-CTLA4 ICI alone and anti-CTLA4 + CD29-PIT (Figure 7(d)). These results suggested that the anti-CTLA4 ICI and anti-CTLA4 + CD29-PIT effectively activated anti-tumor immunity and suppressed cancer cell proliferation.

Discussion

We used two low doses of NIR light irradiation for most of the *in vivo* experiments. Delivered in this way, both CD29-PIT and CD44-PIT resulted in much more cell killing than with a single dose of light. This may be related to increased permeability of the vessels after the first PIT session which allows better distribution of the AbPC prior to the 2nd light application. This is a well-known effect of NIR-PIT and is known as the super-enhanced permeability and retention (SUPR) effect. With the

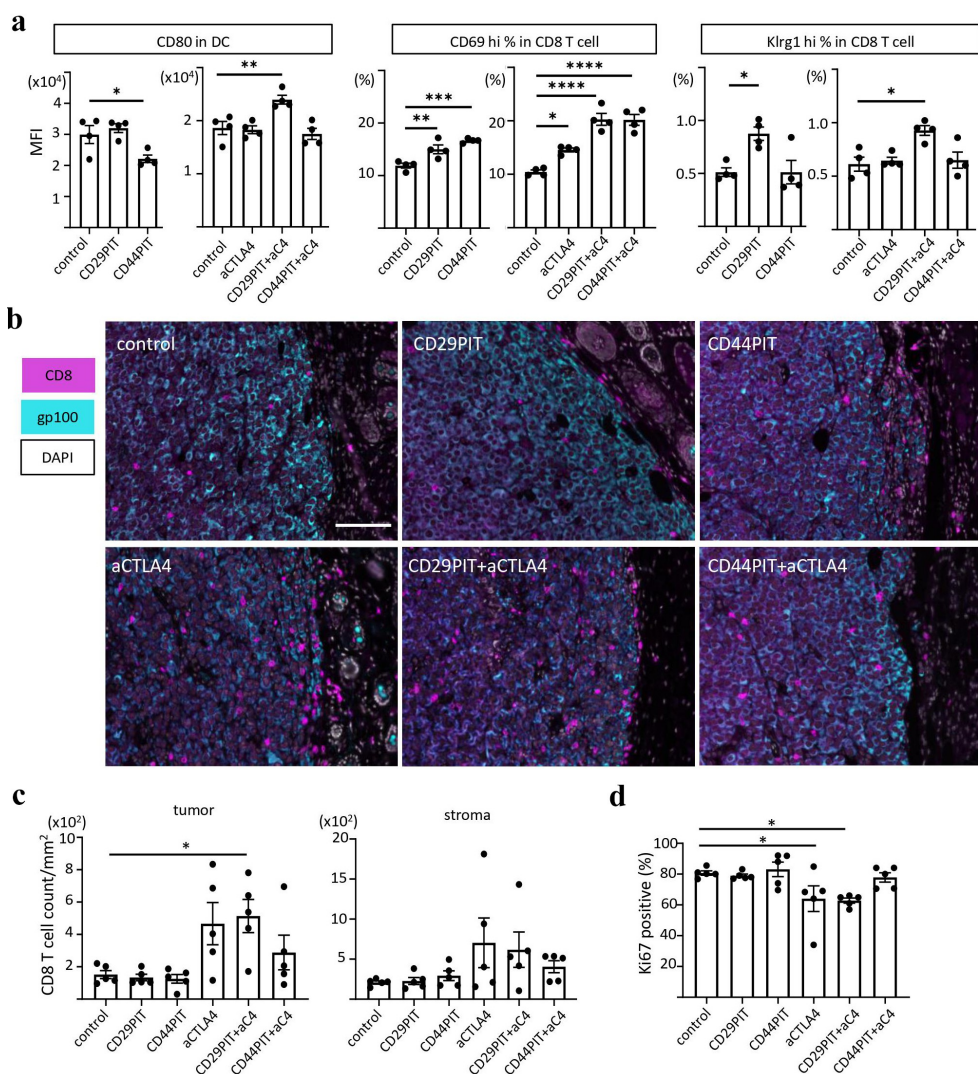


Figure 7. Immuno-activation after CD29-PIT and CD44-PIT in B16 tumor model. (a) The expressions of immune activation markers were analyzed by flow cytometry in tumor-draining lymph nodes on day 2 (1 day after 2nd NIR light irradiation). Expression of DC maturation marker CD80 in DC cells are shown in MFI, T cell activation marker CD69 and effector T cell differentiation marker Klrp1 in CD8 T cell are shown as a positive percentage. Control = no treatment; aCTLA4 = anti-CTLA4 administration only; CD29PIT+aC4 and CD44PIT+aC4 = anti-CTLA4 administration plus CD29-PIT or CD44-PIT. n = 5 (individual tumors), **p* < .05; ***p* < .01; ****p* < .001; *****p* < .0001 (vs control, one-way ANOVA followed by Tukey test) (b-d) Tumor microenvironment was analyzed by IHC on day 7 (6 days after 2nd NIR light irradiation). (b) Representative images of CD8 T cell distribution. The B16 melanoma cells were stained with gp100 IHC (shown in cyan) to mark the tumor tissue. Scale bar = 100 μ m. (c) CD8 T cell count in tumor and stroma counted from IHC, shown as count/mm². n = 5 (individual tumors), **p* < .05 (vs control, one-way ANOVA followed by Tukey test) (d) Ki67 positive percentage in B16 melanoma cells. n = 5 (individual tumors), **p* < .05 (vs control, one-way ANOVA followed by Tukey test).

SUPR effect, the part of tumor tissue, which did not have enough AbPC bound on the cell surface at the time of the 1st irradiation could receive “fresh” AbPC by the time of the 2nd irradiation. Also, keeping NIR light dose low would be beneficial to avoid nonspecific tissue damage because high-dose NIR light (above 600 mW/cm²) by itself is known to cause tissue damage.³⁷ Even with two exposures of NIR light, CD44-PIT rarely destroyed tumors far from the surface. This is likely because the expression of CD44 on the B16 tumor was the weakest on the surface, and the first NIR light irradiation of CD44-PIT did not result in a sufficient SUPR effect to allow for deeper AbPC penetration within the tumor prior to the 2nd exposure of NIR light. In addition to robust tumor shrinkage immediately after the CD29-PIT, regrowth of tumors treated with CD29-PIT was slower. This was thought to be because CD29-PIT preferentially killed the most proliferative subpopulation of cancer cells. Since cancer cells in tumors are heterogeneous, targeting the most proliferative subset is beneficial for prolonging intervals between treatments. Nonetheless, there were often surviving tumor cells, which eventually regrew, after CD29- and CD44-PIT in B16 tumor. Based on the expression pattern of the target antigen in the PIT-surviving tumor cells, this may be the result of the heterogeneity of antigen expression, including cellular localization. Targeting multiple targets, ideally, both not expressed in immune cells, by NIR-PIT might help achieve complete cancer cell killing.

This study also showed that while CD29 was expressed on ECs in the vasculature, both CD29-PIT and CD44-PIT killed ECs to some extent. It was unclear if the EC death observed after CD44-PIT was due to direct cell killing or a secondary effect from nearby tissue necrosis. Probably there was low expression of CD44 that was not detectable by IHC but enough to induce cell death by CD44-PIT. While EC death was observed, the blood vessels were maintained on histology and seemed to be functional based on a marked SUPR effect. This probably is because blood vessels are not solely composed of ECs but are supported by basal membrane and pericytes. There have been several examples of vascular-targeted NIR-PIT which were intended to shut down intra-tumoral blood supply and while reducing blood flow did not eliminate it.^{38,39} Tumor vasculature is an important source of activated immune cells. Therefore, in the cases in which anti-tumor immune activation is included in the therapy mechanism like in this study, leaving intra-tumoral vessels intact may be of benefit. Also, when high-dose NIR light was applied, we observed some adverse events such as paralysis of the limb on the treated side, which might be a sign of vascular or nerve damage. For these reasons, we concluded it is beneficial to perform CD29-PIT with low-dose NIR light. Since we observed the increase of newly activated CD8 T cells in the tumor after CD29-PIT combined with anti-CTLA4 ICI, the vessels were likely to be functional enough to support the transport of newly activated T cells to the treated tumor.

NIR-PIT did not cause damage to adjacent normal skin. Intravenously administrated mAb rarely penetrated the epidermis, and CD29-PIT and CD44-PIT showed no effect on normal skin, providing a margin of safety for its use. However,

a caveat is that NIR-PIT may not be effective against early-stage melanomas that do not penetrate into the dermis as AbPC delivery to the epidermis is limited. For such early-stage skin cancers, other methods of AbPC administration, for instance, topical ointments, might be necessary. NIR-PIT is expected to be more effective against advanced-stage melanomas, which penetrate the dermis.

Although DIG-labeled antibodies were widely distributed in the dermis, no notable increase in cell death was observed. This antibody distribution was thought to be nonspecific, likely representing trapping in the extracellular matrix. These unbound AbPC are expected to have no biological effect and do not affect treatment.

A consequence of direct cell killing by NIR-PIT is induced host cell immunity, which increases the effectiveness of the treatment. CD8 T cell activation relies on DCs, which capture antigens released from killed cancer cells, migrate to the LNs and undergo maturation, whereupon cDC1 cells activate CD8 T cells and cDC2 activate CD4 T cells, which together have a profound anti-cancer effect⁴⁰ in combination with NK cells that also attack cancer cells. Ideally, a treatment intended to rely on an immune response should not damage these immune cells. The *ex-vivo* PIT showed that CD29-PIT does not damage intratumoral immune cells while CD44-PIT significantly reduced CD4 T cells, NK cells, and cDC2 due to their expression of CD44. Our previous study showed CD44-PIT destroyed CD44-positive activated CD8 T cells¹⁵ working counter-productively against the intent of the treatment. In this study, there was no significant reduction of CD8 T cells, likely because few CD8 T cells were activated upon the treatment in the B16 tumor model. Even if some T cells were killed at the treatment site, this might not be critical because newly activated T cells will be supplied from the tumor-draining LNs, which are outside the treatment zone. However, DCs capture antigens released from destroyed cancer cells then carry them to the LNs and present the antigen to activate T cells, so, the loss of DCs by CD44-PIT might be more critical than the loss of CD8 T cells.

Besides CD44-PIT, its isotype control IgG2b-PIT also slightly reduced NK cells and cDC2. This may be because these cells express Fc receptors to which the antibody binds. The isotype control of anti-CD29, rat IgG2a PIT did not kill these cells. The difference in properties, such as the affinity of FcR binding or amount of nonspecific binding might be different between the two isotypes and, therefore, affect the NK and cDC2 killing efficacy by NIR-PIT.

Since CD29-PIT keeps immune cell populations intact, we hypothesized that the anti-tumor efficacy of CD29-PIT might be augmented by ICI, especially by anti-CTLA4 which prevents the blocking of DC-mediated T cell activation.^{41,42} Two days after the first NIR light irradiation, although the number of tumor-infiltrating CD8 T cells was not significantly different between anti-CTLA4 ICI alone and CD29-PIT + anti-CTLA4 ICI, CD29-PIT + anti-CTLA4 ICI did increase the expression of the DC maturation marker, CD69 positive activated CD8 T cells, Klrp1 positive effector CD8 T cells while CD8 T cell infiltration was also increased. This result suggests that the combination of CD29-PIT with anti-CTLA4 ICI augmented T cell activation and effector differentiation, which would lead to more effective tumor suppression. In comparison, CD44-PIT slightly reduced DC maturation marker expression. Although

CD8 T cell activation occurred similarly as after the CD29-PIT, no increase in effector marker expression nor significant increase of T cell infiltration was observed after CD44-PIT. These results suggest that initial CD8 T cell activation occurred, but effector differentiation was less successful after CD44-PIT than it was for CD29-PIT. Whereas CD29-PIT preserved immune cells that support CD8 T cell activation, CD44-PIT largely reduced these cells. While the tumor could replenish these cells from nearby tissue, however, even transient loss might have affected the T cell activation after the CD44-PIT. Despite the partial loss of immune cells, our previous study in other tumor models showed that CD44-PIT could increase the CD8 T cell infiltration in combination with ICI. However, targets such as CD29 that directly kill tumor cells but do not affect immune cells are more effective and can be more successfully combined with other immunotherapies such as immune checkpoint inhibitors.

This study had several limitations. Only one melanoma cell line was used to test the efficacy of CD29-PIT and CD44-PIT. Additional cell lines will be tested in the future. Additionally, while the anti-CTLA4 ICI and CD29-PIT combination significantly extended survival, it was not efficient enough to achieve cures. In this study, we administered anti-CTLA4 ICI during the first one week of treatment, extending this period may improve anti-tumor efficacy. For the later phase of treatment, anti-PD-1 ICI which upregulates effector function and is widely used for melanoma treatment may help improve long-term survival. Alternatively, combining both anti-CTLA4 and anti-PD-1 ICIs with NIR-PIT would be interesting since this combination is commonly used in clinical settings. Additional combination therapies such as activation cytokine IL-15 or CTLA4-PIT that can eliminate suppressor cells^{43,44} may also lead to improved efficacy, however, these remain to be tested.

Conclusion

In this study, we showed NIR-PIT is effective against pigmented melanomas and shows no difference when compared to non-pigmented tumors with similar target expression profiles. CD29-PIT was more effective than CD44-PIT in shrinking B16 melanomas. Unlike CD44-PIT, CD29-PIT did not destroy immune cells at the treatment site, enabling a more robust immune response. Moreover, the combination of CD29-PIT with anti-CTLA4 ICI was highly effective. CD29 is expressed in various cancers, so it may be a promising treatment against a wide variety of cancers besides melanoma, especially in combination with other immunotherapies such as checkpoint inhibitors to maximize its treatment effect.

Disclosure statement

No potential conflict of interest was reported by the author(s).

Funding

This work was supported by the Intramural Research Program of the National Institutes of Health, National Cancer Institute, Center for Cancer Research [grant number ZIA BC 011513]; National Center for Global Health and Medicine.

ORCID

Aki Furusawa  <http://orcid.org/0000-0002-1339-4219>

References

1. Kobayashi H, Choyke PL. Near-infrared photoimmunotherapy of cancer. *Acc Chem Res.* 2019;52(8):2332–2339. doi:10.1021/acs.accounts.9b00273.
2. Wei W, Jiang D, Ehlerding EB, Barnhart TE, Yang Y, Engle JW, Luo Q-Y, Huang P, Cai W. CD146-targeted multimodal image-guided photoimmunotherapy of Melanoma. *Adv Sci (Weinh).* 2019;6(9):1801237. doi:10.1002/advs.201801237.
3. Mallidi S, Anbil S, Bulin AL, Obaid G, Ichikawa M, Hasan T. Beyond the barriers of light penetration: strategies, perspectives and possibilities for photodynamic therapy. *Theranostics.* 2016;6(13):2458–2487. doi:10.7150/thno.16183.
4. McClain SE, Mayo KB, Shada AL, Smolkin ME, Patterson JW, Slingluff CL Jr. Amelanotic melanomas presenting as red skin lesions: a diagnostic challenge with potentially lethal consequences. *Int J Dermatol.* 2012;51(4):420–426. doi:10.1111/j.1365-4632.2011.05066.x.
5. Kobayashi H, Furusawa A, Rosenberg A, Choyke PL. Near-infrared photoimmunotherapy of cancer: a new approach that kills cancer cells and enhances anti-cancer host immunity. *Int Immunol.* 2021;33(1):7–15. doi:10.1093/intimm/dxaa037.
6. Li L, Hao X, Qin J, Tang W, He F, Smith A, Zhang M, Simeone DM, Qiao XT, Chen Z-N, et al. Antibody against CD44s inhibits pancreatic tumor initiation and postradiation recurrence in mice. *Gastroenterology.* 2014;146(4):1108–1118. doi:10.1053/j.gastro.2013.12.035.
7. Hong SP, Wen J, Bang S, Park S, Song SY. CD44-positive cells are responsible for gemcitabine resistance in pancreatic cancer cells. *Int J Cancer.* 2009;125(10):2323–2331. doi:10.1002/ijc.24573.
8. Brown RL, Reinke LM, Damerow MS, Perez D, Chodosh LA, Yang J, Cheng C. CD44 splice isoform switching in human and mouse epithelium is essential for epithelial-mesenchymal transition and breast cancer progression. *J Clin Invest.* 2011;121(3):1064–1074. doi:10.1172/JCI44540.
9. Zoller M. CD44: can a cancer-initiating cell profit from an abundantly expressed molecule? *Nat Rev Cancer.* 2011;11(4):254–267. doi:10.1038/nrc3023.
10. Li C, Heidt DG, Dalerba P, Burant CF, Zhang L, Adsay V, Wicha M, Clarke MF, Simeone DM. Identification of pancreatic cancer stem cells. *Cancer Res.* 2007;67(3):1030–1037. doi:10.1158/0008-5472.CAN-06-2030.
11. Nagaya T, Nakamura Y, Okuyama S, Ogata F, Maruoka Y, Choyke PL, Allen C, Kobayashi H. Syngeneic mouse models of oral cancer are effectively targeted by anti-CD44-based NIR-PIT. *Mol Cancer Res.* 2017;15(12):1667–1677. doi:10.1158/1541-7786.MCR-17-0333.
12. Maruoka Y, Furusawa A, Okada R, Inagaki F, Fujimura D, Wakiyama H, Kato T, Nagaya T, Choyke PL, Kobayashi H, et al. Combined CD44- and CD25-targeted near-infrared photoimmunotherapy selectively kills cancer and regulatory T cells in syngeneic mouse cancer models. *Cancer Immunol Res.* 2020;8(3):345–355. doi:10.1158/2326-6066.CIR-19-0517.
13. Jin J, Krishnamachary B, Mironchik Y, Kobayashi H, Bhujwala ZM. Phototheranostics of CD44-positive cell populations in triple negative breast cancer. *Sci Rep.* 2016;6(1):27871. doi:10.1038/srep27871.
14. Termeer C, Johannsen H, Braun T, Renkl A, Ahrens T, Denfeld RW, Lappin MB, Weiss JM, Simon JC. The role of CD44 during CD40 ligand-induced dendritic cell clustering and maturation. *J Leukoc Biol.* 2001;70:715–722.
15. Maruoka Y, Furusawa A, Okada R, Inagaki F, Fujimura D, Wakiyama H, Kato T, Nagaya T, Choyke PL, Kobayashi H, et al. Near-infrared photoimmunotherapy combined with CTLA4 checkpoint blockade in syngeneic mouse cancer models. *Vaccines (Basel).* 2020;8(3). doi:10.3390/vaccines8030528.

16. Wakiyama H, Furusawa A, Okada R, Inagaki F, Kato T, Maruoka Y, Choyke PL, Kobayashi H. Increased immunogenicity of a minimally immunogenic tumor after cancer-targeting near infrared photoimmunotherapy. *Cancers (Basel)*. 2020;12(12):3747. doi:10.3390/cancers12123747.
17. Maruoka Y, Furusawa A, Okada R, Inagaki F, Wakiyama H, Kato T, Nagaya T, Choyke PL, Kobayashi H. Interleukin-15 after Near-Infrared Photoimmunotherapy (NIR-PIT) enhances T cell response against syngeneic mouse tumors. *Cancers (Basel)*. 2020;12(9):2575. doi:10.3390/cancers12092575.
18. Desgrosellier JS, Cheresh DA. Integrins in cancer: biological implications and therapeutic opportunities. *Nat Rev Cancer*. 2010;10(1):9–22. doi:10.1038/nrc2748.
19. Geng S, Guo Y, Wang Q, Li L, Wang J. Cancer stem-like cells enriched with CD29 and CD44 markers exhibit molecular characteristics with epithelial-mesenchymal transition in squamous cell carcinoma. *Arch Dermatol Res*. 2013;305(1):35–47. doi:10.1007/s00403-012-1260-2.
20. Meenakshi Sundaram DN, Kucharski C, Parmar MB, Kc RB, Uludag H. Polymeric delivery of siRNA against integrin-beta1 (CD29) to reduce attachment and migration of breast cancer cells. *Macromol Biosci*. 2017;17(6):1600430. doi:10.1002/mabi.201600430.
21. Yao ES, Zhang H, Chen YY, Lee B, Chew K, Moore D, Park C. Increased $\beta 1$ integrin is associated with decreased survival in invasive breast cancer. *Cancer Res*. 2007;67(2):659–664. doi:10.1158/0008-5472.CAN-06-2768.
22. Zhou Y, Chen D, Qi Y, Liu R, Li S, Zou H, Lan J, Ju X, Jiang J, Liang W, et al. Evaluation of expression of cancer stem cell markers and fusion gene in synovial sarcoma: insights into histogenesis and pathogenesis. *Oncol Rep*. 2017;37(6):3351–3360. doi:10.3892/or.2017.5617.
23. Pandolfi F, Trentin L, Boyle LA, Stamenkovic I, Byers HR, Colvin RB, Kurnick JT. Expression of cell adhesion molecules in human melanoma cell lines and their role in cytotoxicity mediated by tumor-infiltrating lymphocytes. *Cancer*. 1992;69(5):1165–1173. doi:10.1002/cncr.2820690517.
24. Contador-Troca M, Alvarez-Barrientos A, Merino JM, Morales-Hernandez A, Rodriguez MI, Rey-Barroso J, Barrasa E, Cerezo-Guisado MI, Catalina-Fernández I, Sáenz-Santamaría J, et al. Dioxin receptor regulates aldehyde dehydrogenase to block melanoma tumorigenesis and metastasis. *Mol Cancer*. 2015;14(1):148. doi:10.1186/s12943-015-0419-9.
25. Nicolet BP, Guislain A, van Alphen FPJ, Gomez-Eerland R, Schumacher TNM, van Den Biggelaar M, Wolkers MC. CD29 identifies IFN- γ -producing human CD8+ T cells with an increased cytotoxic potential. *Proc Natl Acad Sci U S A*. 2020;117(12):6686–6696. doi:10.1073/pnas.1913940117.
26. Uhlen M, Fagerberg L, Hallstrom BM, Lindskog C, Oksvold P, Mardinoglu A, Sivertsson Å, Kampf C, Sjöstedt E, Asplund A, et al. Proteomics. Tissue-based map of the human proteome. *Science*. 2015;347(6220):1260419. doi:10.1126/science.1260419.
27. Miller MAZ, F J. Mechanisms and morphology of cellular injury, adaptation, and death. In: Zachary JF, editor. *pathologic basis of veterinary disease*. 6ed. Amsterdam: Elsevier Inc.;2017. p.2–43.e19.
28. Kobayashi H, Choyke PL. Super enhanced permeability and retention (SUPR) effects in tumors following near infrared photoimmunotherapy. *Nanoscale*. 2016;8(25):12504–12509. doi:10.1039/c5nr05552k.
29. Goncharov NV, Nadeev AD, Jenkins RO, Avdonin PV. Markers and biomarkers of endothelium: When something is rotten in the State. *Oxid Med Cell Longev*. 2017;2017:9759735. doi:10.1155/2017/9759735.
30. Cao G, Savani RC, Fehrenbach M, Lyons C, Zhang L, Coukos G, DeLisser HM. Involvement of endothelial CD44 during in vivo angiogenesis. *Am J Pathol*. 2006;169(1):325–336. doi:10.2353/ajpath.2006.060206.
31. Bata-Csorgo Z, Hammerberg C, Voorhees JJ, Cooper KD. Flow cytometric identification of proliferative subpopulations within normal human epidermis and the localization of the primary hyperproliferative population in psoriasis. *J Exp Med*. 1993;178(4):1271–1281. doi:10.1084/jem.178.4.1271.
32. Tuhkanen AL, Agren UM, Tammi MI, Tammi RH. CD44 expression marks the onset of keratinocyte stratification and mesenchymal maturation into fibrous dermis in fetal human skin. *J Histochem Cytochem*. 1999;47(12):1617–1624. doi:10.1177/002215549904701213.
33. Shatirishvili M, Burk AS, Franz CM, Pace G, Kastilan T, Breuhahn K, Hinterseer E, Dierich A, Bakiri L, Wagner EF, et al. Epidermal-specific deletion of CD44 reveals a function in keratinocytes in response to mechanical stress. *Cell Death Dis*. 2016;7(11):e2461. doi:10.1038/cddis.2016.342.
34. Peuhu E, Salomaa SI, De Franceschi N, Potter CS, Sundberg JP, Pouwels J, Gullberg D. Integrin beta 1 inhibition alleviates the chronic hyperproliferative dermatitis phenotype of SHARPIN-deficient mice. *PLoS One*. 2017;12(10):e0186628. doi:10.1371/journal.pone.0186628.
35. Moreno-Layseca P, Icha J, Hamidi H, Ivaska J. Integrin trafficking in cells and tissues. *Nat Cell Biol*. 2019;21(2):122–132. doi:10.1038/s41556-018-0223-z.
36. Nakajima K, Ogawa M. Phototoxicity in near-infrared photoimmunotherapy is influenced by the subcellular localization of antibody-IR700. *Photodiagnosis Photodyn Ther*. 2020;31:101926. doi:10.1016/j.pdpdt.2020.101926.
37. Okuyama S, Nagaya T, Ogata F, Maruoka Y, Sato K, Nakamura Y, Choyke PL, Kobayashi H. Avoiding thermal injury during near-infrared photoimmunotherapy (NIR-PIT): the importance of NIR light power density. *Oncotarget*. 2017;8(68):113194–113201. doi:10.18632/oncotarget.20179.
38. Nishimura T, Mitsunaga M, Ito K, Kobayashi H, Saruta M. Cancer neovasculature-targeted near-infrared photoimmunotherapy (NIR-PIT) for gastric cancer: different mechanisms of phototoxicity compared to cell membrane-targeted NIR-PIT. *Gastric Cancer*. 2020;23(1):82–94. doi:10.1007/s10120-019-00988-y.
39. Bao R, Wang Y, Lai J, Zhu H, Zhao Y, Li S, Li N, Huang J, Yang Z, Wang F, et al. Enhancing anti-PD-1/PD-L1 immune checkpoint inhibitory cancer therapy by CD276-targeted photodynamic ablation of tumor cells and tumor vasculature. *Mol Pharm*. 2019;16(1):339–348. doi:10.1021/acs.molpharmaceut.8b00997.
40. Borst J, Ahrends T, Babala N, Melief CJM, Kastenmuller W. CD4+ T cell help in cancer immunology and immunotherapy. *Nat Rev Immunol*. 2018;18(10):635–647. doi:10.1038/s41577-018-0044-0.
41. Seidel JA, Otsuka A, Kabashima K. Anti-PD-1 and anti-CTLA-4 therapies in cancer: mechanisms of action, efficacy, and limitations. *Front Oncol*. 2018;8:86. doi:10.3389/fonc.2018.00086.
42. Waldman AD, Fritz JM, Lenardo MJ. A guide to cancer immunotherapy: from T cell basic science to clinical practice. *Nat Rev Immunol*. 2020;20(11):651–668. doi:10.1038/s41577-020-0306-5.
43. Okada R, Kato T, Furusawa A, Inagaki F, Wakiyama H, Choyke PL, Kobayashi H. Local depletion of immune checkpoint ligand CTLA4 expressing cells in tumor beds enhances antitumor host immunity. *Adv Ther (Weinh)*. 2021;4(5). doi:10.1002/adtp.202000269.
44. Kato T, Okada R, Furusawa A, Inagaki F, Wakiyama H, Furumoto H, Okuyama S, Fukushima H, Choyke PL, Kobayashi H, et al. Simultaneously combined cancer cell- and CTLA4-targeted NIR-PIT causes a synergistic treatment effect in syngeneic mouse models. *Mol Cancer Ther*. 2021;20(11):2262–2273. doi:10.1158/1535-7163.MCT-21-0470.